

A Model-Based Control of Self-Driving Car Trajectory for Lanes Change Maneuver in a Smart City

IGOR ASTROV

Department of Software Science,
Tallinn University of Technology,
Akadeemia tee 15a, 12618, Tallinn,
ESTONIA

Abstract: - High-quality computer control of autonomous vehicles in various environments is a priority for cyber-physical systems (CPS), Industry 4.0, and the global economy as a whole. The paper discusses the linearized control model of a Self-Driving Car (SDC) with a weight of 1160 kg. For safe maneuvering with obstacle avoidance, we employ an optimal control by Linear Quadratic Regulator (LQR) using a Simulink/MATLAB environment that is capable to demonstrate the satisfiability of LQR control for this maneuver using a 3D simulation environment under changing urban conditions in a smart city. This controller is easy for engineering implementation.

Key-Words: - bicycle model, computer simulation, LQR control, mathematical model, self-driving cars, smart city.

Received: December 28, 2022. Revised: September 2, 2023. Accepted: October 7, 2023. Published: October 27, 2023.

1 Introduction

Unmanned autonomous vehicles (AVs) are becoming increasingly important in CPS, Industry 4.0, and the global economy as a whole, [1]. AV needs to be developed and applied using mathematical models that should replace the ordinary mental models that have developed in the head of a human driver of conventional vehicles, [2].

In Tallinn University of Technology (TalTech), during a noticeable time one of the priority study fields has been the research of SDCs, [3], [4], [5]. Modeling and simulation for very different types of aerial AVs and aquatic (both underwater and surface) AVs have been a notable research theme for several years now, [6], [7], [8], [9]. These activities have recently been included in the development of the Smart City environment, which expands the cooperation concept for the twin city Tallinn-Helsinki, [10], [11].

Urban AVs in Smart Cities operate in a higher range of speeds and accelerations than commonly used mobile robots. This fact necessitates the use of dynamic systems techniques to make the control safer and smoother.

To achieve autonomous motion in driving a series of components are necessary. First, an AV sensor network collects all information about the AV and environment and makes the necessary measurements. Secondly, the trajectory planning

component generates the desired travel route using the actual and desired position of the AV. Finally, the automatic control system generates control actions on the drives.

Reliable operation of the automatic control system is one of the most important tasks for AV because it guarantees its autonomous motion. Therefore, it is necessary to use rigorous mathematical models of AV.

The problems of traffic planning and control are two different, but closely related tasks for SDCs. The first task is to calculate the possible trajectory of the vehicle avoiding surrounding obstacles such as pedestrians, other vehicles, or nonmoving objects. The second task is the impact on the executive mechanisms (accelerator pedal, brake pedal, and steering wheel) to follow the trajectory obtained by the motion planner, while the system maintains stability and, if possible, a smooth ride.

It is assumed that the trajectory set by the traffic planner is safe within certain limits, and then the goal of the controller is to follow the given safe trajectory as best as possible, without considering obstacles. If the controller fails to follow safe trajectories, it will the entire system in jeopardy.

This work aims to create a mathematical model of SDC ISEAUTO and implement a control system for the resulting model in the Simulink environment

by the guidelines of the allocated grant for these studies.

The level of complexity of the task of controlling the guidance of a vehicle can be characterized by two facets: the type of control (lateral, longitudinal, or mixed) and the complexity of the used model (kinematic, linear-dynamic, or non-linear dynamic). This article deals with complex configurations for solving a nonlinear dynamic problem. Here, we model a custom-designed LQR control system that uses the initial non-linear dynamic model of the SDC.

The LQR controller is chosen here as the most suitable for the obtained mathematical model of the SDC with many inputs and many outputs, as well as for a simpler obtaining of the output trajectory without additional transformations. This LQR approach greatly reduces the computational cost for real-time operation because it works in a much faster way. This article shows the neat efficiency of the output coordinate stabilization task.

2 Nonlinear Model of SDC

The bicycle model was used to simulate the SDC to receive the desired accuracy and avoid expensive computational costs.

As stated in Figure 1, the transverse dynamics and longitudinal dynamics have been considered.

The bicycle model is obtained from a four-wheeled SDC by gluing the front and rear wheels into a single front and rear wheel, respectively, along the longitudinal axis of the SDC without the inclusion of pitch and roll dynamics.

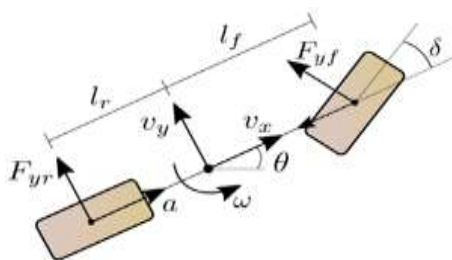


Fig. 1: Bicycle model

The goal is to be able to control the SDC's trajectory to reach the desired position as fast and safely as possible.

The kinematics of SDC can be represented in the form of such equations, as, [12].

$$\dot{x} = v_x \cos \theta - v_y \sin \theta \quad (1)$$

$$\dot{y} = v_x \sin \theta + v_y \cos \theta \quad (2)$$

$$\dot{\theta} = \omega \quad (3)$$

where x, y are the coordinates of the center of mass in the earth-fixed frame, respectively, θ is the yaw angle, v_x, v_y are the longitudinal and lateral speeds in the body frame, respectively, and ω is the yaw rate.

The bicycle model of SDC can be described by the following equations, [13].

$$m\dot{v}_x = F_x + mv_y\omega \quad (4)$$

$$m\dot{v}_y = -mv_x\omega + 2(F_{yf} \cos \delta + F_{yr}) \quad (5)$$

$$I\dot{\omega} = 2(l_f F_{yf} \cos \delta - l_r F_{yr}) \quad (6)$$

where m is the mass, I is the yaw inertia, F_{yf} and F_{yr} are the lateral tire forces of the front and rear wheels, respectively; F_x is the driving force, δ is the front steering angle; l_f and l_r are the distances from the center of mass to the front and rear wheel axes, respectively.

The driving force F_x in (4) can be written as

$$F_x = ma \quad (7)$$

where a is an acceleration.

The forces F_{yf} and F_{yr} can be found so, [12]

$$F_{yf} = C_f \left(\delta - \tan^{-1} \left(\frac{v_y + l_f \dot{\theta}}{v_x} \right) \right) \quad (8)$$

$$F_{yr} = -C_r \tan^{-1} \left(\frac{v_y - l_r \dot{\theta}}{v_x} \right) \quad (9)$$

where the C_f and C_r are the constant tire stiffness parameters.

The coordinates and yaw angle can be found by integrating

$$x(\tau) = \int_0^\tau \dot{x}(t) dt, y(\tau) = \int_0^\tau \dot{y}(t) dt,$$

$$\theta(\tau) = \int_0^\tau \dot{\theta}(t) dt, \quad (10)$$

It can be seen that the vector drawn up of coordinates and yaw angle can be calculated from obtained equations (1)-(10).

3 Parameters of the Nonlinear Model of SDC

It is known that some parameters of the SDK strongly depend on environmental conditions. Therefore, even small changes in these parameters can significantly affect the movement of the SDK.

As a result, for example, the estimation of the values of parameters of SDC for the needs of accident reconstruction is very important.

The main parameters of such SDC as ISEAUTO, [14], are calculated here.

The following parameters of this vehicle are known

$$m = 1160 \text{ kg}, l_f = 1.275 \text{ m}, l_r = 1.275 \text{ m}$$

The moment of inertia I was calculated so, [15]:

$$I = \frac{m}{12} (l_x^2 + l_y^2) \quad (11)$$

Hence, assuming that length $l_x = 3.6 \text{ m}$ and width $l_y = 1.5 \text{ m}$, from (11), we find

$$I = 1470.3 \text{ kgm}^2$$

Now it is necessary to evaluate the values of C_f and C_r .

Assuming a small yaw angle θ in a stable state, we find

$$v_x \approx \text{const}, v_y \approx 0 \quad (12)$$

The yaw rate can be obtained in this way, [16]

$$\dot{\theta} = \frac{v_x}{(l_f + l_r)} \tan \delta \quad (13)$$

From (8), (9), (12), and (13), we find

$$F_{yf} = C_f \left(\delta - \tan^{-1} \left(\frac{l_f \tan \delta}{l_f + l_r} \right) \right) \quad (14)$$

$$F_{yr} = C_r \tan^{-1} \left(\frac{l_r \tan \delta}{l_f + l_r} \right) \quad (15)$$

The next inequalities can be done

$$0 < \frac{l_f}{l_f + l_r} < 1 \quad (16)$$

$$0 < \frac{l_r}{l_f + l_r} < 1 \quad (17)$$

Assuming that we have a small angle of rotation δ in the stable state, using that $\tan^{-1}(\tan x) = x$, and (14)-(17), we get

$$F_{yf} = \frac{C_f l_r \delta}{l_f + l_r} \quad (18)$$

$$F_{yr} = \frac{C_r l_r \delta}{l_f + l_r} \quad (19)$$

Assuming that we have a small constant yaw angle θ and a small steering angle δ in a stable state, we get

$$\cos \delta \approx 1, \dot{\omega} \approx 0 \quad (20)$$

Combining (6) and (20), we obtain

$$l_f F_{yf} \approx l_r F_{yr} \quad (21)$$

Combining (18)-(19) and (21), we obtain

$$C_r \approx \frac{l_f}{l_r} C_f \quad (22)$$

Assuming that we have a small steering angle δ and v_y is constant in a stable state, we get

$$\cos \delta \approx 1, \dot{v}_y \approx 0 \quad (23)$$

Combining (5) and (27), we obtain

$$m v_x \omega \approx 2 F_{yf} + 2 F_{yr} \quad (24)$$

From (3), (13), (18), (19), (22), and (24), and assuming that we have a small $\tan \delta \approx \delta$ at stable state, we get

$$C_f \approx \frac{m v_x^2}{2(l_f + l_r)} \quad (25)$$

The vehicle's path depends on many parameters, including tire, vehicle, and road characteristics. For example, the stiffness of a wheel in a turn changes from 50% to 150% of the calculated value, [16].

Consequently, the maximum ratio of C_f from (25) becomes:

$$C_{fmax} \approx \frac{m v_{xmax}^2}{2(l_f + l_r)} \quad (26)$$

where v_{xmax} is a maximum of velocity v_x .

Hence, from (22), (26) and assuming that $v_{xmax} = 50 \text{ km/h}$, we find

$$C_f = 43875 \frac{N}{rad}, C_r = 43875 \frac{N}{rad}$$

4 State-Space Model of SDC

From (4) and (7), we find

$$\dot{v}_x = a + v_y \omega \quad (27)$$

It is possible to consider v_y, ω as small values then $v_y \omega$ is a negligible value at a stable state, and from (27), we obtain

$$\dot{v}_x \approx a \quad (28)$$

Also, it is possible to consider the a as a zero in (28), i.e.

$$v_x = V_c \quad (29)$$

where V_c is a fixed constant.

We linearize (1)-(2) by using the Taylor series. From (1), (2), and (29), we find

$$\dot{x} = V_c - v_y \theta \quad (30)$$

$$\dot{y} = V_c \theta + v_y \quad (31)$$

The lateral tire force for front wheels F_{yf} and the lateral tire force for the rear wheels F_{yr} can be calculated so, [12]

$$F_{yf} = C_f \left(\delta - \frac{v_y + l_f \omega}{v_x} \right) \quad (32)$$

$$F_{yr} = -C_r \left(\frac{v_y - l_r \omega}{v_x} \right) \quad (33)$$

Combining (29) and (32)-(33), we obtain

$$F_{yf} = C_f \delta - \frac{C_f v_y}{V_c} - \frac{C_f l_f \omega}{V_c} \quad (34)$$

$$F_{yr} = -\frac{C_r v_y}{V_c} + \frac{C_r l_r \omega}{V_c} \quad (35)$$

From (5), (34), (35), and believing that $\cos \delta \approx 1$ at stable state, we obtain

$$\dot{v}_y = \frac{2C_f}{m} \delta - \frac{2(C_f + C_r)}{mV_c} v_y + \left(\frac{2(C_r l_r - C_f l_f)}{mV_c} - V_c \right) \omega \quad (36)$$

From (6), (34), (35), and believing that $\cos \delta \approx 1$ at stable state, we obtain

$$\dot{\omega} = \frac{2C_f l_f}{I} \delta + \frac{2(C_r l_r - C_f l_f)}{IV_c} v_y - \left(\frac{2(C_f l_f^2 + C_r l_r^2)}{IV_c} \right) \omega \quad (37)$$

The state space model of SDC has the next form

$$\dot{X} = AX + BU \quad (38)$$

$$Y = CX + DU \quad (39)$$

Then, the state vector and input signal are defined so

$$X = \begin{bmatrix} y \\ v_y \\ \omega \\ \theta \end{bmatrix}, U = \delta \quad (40)$$

The matrix A in (38) can be described as

$$A = \begin{bmatrix} 0 & 1 & 0 & V_c \\ 0 & a_{22} & a_{23} & 0 \\ 0 & a_{32} & a_{33} & 0 \\ 0 & 0 & 1 & 0 \end{bmatrix} \quad (41)$$

where the next elements of matrix A are obtained from (36)-(37) so

$$a_{22} = -\frac{2(C_f + C_r)}{mV_c}, a_{23} = \frac{2(C_r l_r - C_f l_f)}{mV_c} - V_c,$$

$$a_{32} = \frac{2(C_r l_r - C_f l_f)}{IV_c}, a_{33} = -\frac{2(C_f l_f^2 + C_r l_r^2)}{IV_c}$$

The matrix B in (38) can be described as

$$B = \begin{bmatrix} 0 \\ b_2 \\ b_3 \\ 0 \end{bmatrix} \quad (42)$$

where the next elements of matrix B are obtained from (36)-(37) so

$$b_2 = \frac{2C_f}{m}, b_3 = \frac{2C_f l_f}{I}$$

The matrices C, D in (39) are denoted so

$$C = \begin{bmatrix} 1 & 0 & 0 & 0 \\ 0 & 1 & 0 & 0 \\ 0 & 0 & 1 & 0 \\ 0 & 0 & 0 & 1 \end{bmatrix}, D = \begin{bmatrix} 0 \\ 0 \\ 0 \\ 0 \end{bmatrix} \quad (43)$$

5 Control System

When the mathematical model of the controlled system is linear and the cost function is quadratic, we have a continuous-time LQR optimal control problem that provides the best possible performance concerning the given cost function.

The problem of LQR control over infinite time for a linear, stationary, stabilized, and detectable model is to calculate the optimal matrix of the feedback coefficients K such that the optimal feedback control law

$$U = -KX \quad (44)$$

minimizes such cost function

$$J = \int (X^T Q X + U^T R U) dt \quad (45)$$

which was applied to (38).

The matrices Q, R in (45) can be chosen by applying the following rules:

$$Q_{ii} = \frac{1}{x_{i \max}^2} \quad (46)$$

$$R_{ii} = \frac{1}{u_{i \max}^2} \quad (47)$$

where $x_{i \max}$ is a maximum acceptable value for the output signal and $u_{i \max}$ is a maximum acceptable value for the input signal.

From (39), (40), (43), (46), and (47), we find

$$Q = \begin{bmatrix} \frac{1}{y_{\max}^2} & 0 & 0 & 0 \\ 0 & \frac{1}{v_y^2 \max} & 0 & 0 \\ 0 & 0 & \frac{1}{\omega^2 \max} & 0 \\ 0 & 0 & 0 & \frac{1}{\theta_{\max}^2} \end{bmatrix}, R = \begin{bmatrix} \frac{1}{\delta_{\max}^2} \end{bmatrix} \quad (48)$$

The matrixes in (48) are chosen so

$$Q = \begin{bmatrix} 0.0400 & 0 & 0 & 0 \\ 0 & 576.0000 & 0 & 0 \\ 0 & 0 & 0.3745 & 0 \\ 0 & 0 & 0 & 25.9382 \end{bmatrix},$$

$$R = [6.4846]$$

6 Simulation Results

In this case, the SDC trajectory consists of two given lines to avoid obstacles.

A block diagram of the control system for the case of velocity $v_x = V_c$ from (29) in Simulink is shown in Figure 2 (Appendix).

The full speed of the vehicle can be found so

$$v = \sqrt{V_c^2 + v_y^2}$$

Let us evaluate the movement restriction area for safe vehicle maneuvers with obstacle avoidance.

Equation of motion under the action of constant velocity $v_x = V_c$ can be expressed so

$$x(t) = V_c t \quad (49)$$

The full-time can be divided into two intervals such as $(0, \tau_1), (\tau_1, \tau_2)$, where these intervals are times for achieving of the reference signal y_{ref1} and reference signal y_{ref2} , respectively.

From (49), we find

$$x_{sd} \approx V_c \tau_1 \quad (50)$$

where x_{sd} is a safe distance.

The prohibited area for movement can be evaluated as a rectangle with a length $l_{rx} \approx x_{sd}$ and a width $l_{ry} \approx y_{ref1} - y_{ref2}$.

The input control signal is determined by the steering angle δ of the front wheel.

The output control signals are determined by v_y , ω , and θ .

Velocity $v_x = 15 \frac{km}{h}$ from (29), the references for coordinate y as $y_{ref1} = 5m, y_{ref2} = 1m$, the setting time $\tau_1 = 54s$ from (50) and the gain matrix from (44) as $K = [0.0785 \ 8.8793 \ 0.0326 \ 3.2515]$ were applied during this maneuver. Note that $x_{sd} = 225m$.

Simulation results for input and output signals are shown in Figure 3 and Figure 5 (Appendix), respectively. The yaw angle for this maneuver is presented in Figure 4. The motion way of SDC is shown in Figure 6. A smooth transition to the desired lines was noticeable without an output signal spike.

Note that the expected accuracy of the output coordinate regulation in Figure 5 (Appendix) lies within 5%, and the resulting accuracy of the output coordinate control in Figure 5 (Appendix) does not exceed 0.19%.

A possible representative form of SDC motion is shown in Figure 7. The Simulation 3D Vehicle block implements three-dimensional animation of a tire force four-wheel SDC. This animation block uses the coordinates and angles of SDC to adjust the rotation for each wheel and make the motion follow the terrain. The Simulation 3D Scene Configuration block implements a virtual 3D simulation environment for the used SDC model.

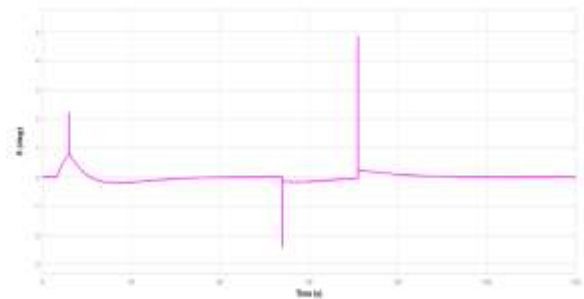


Fig. 3: Steering angle of SDC

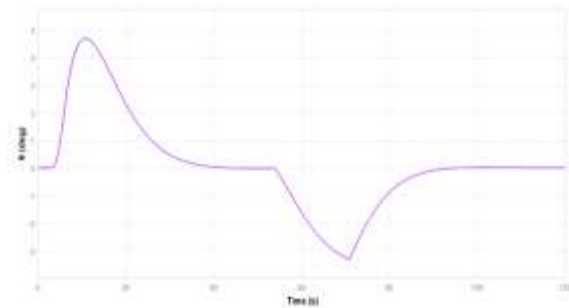


Fig. 4: Yaw angle of SDC

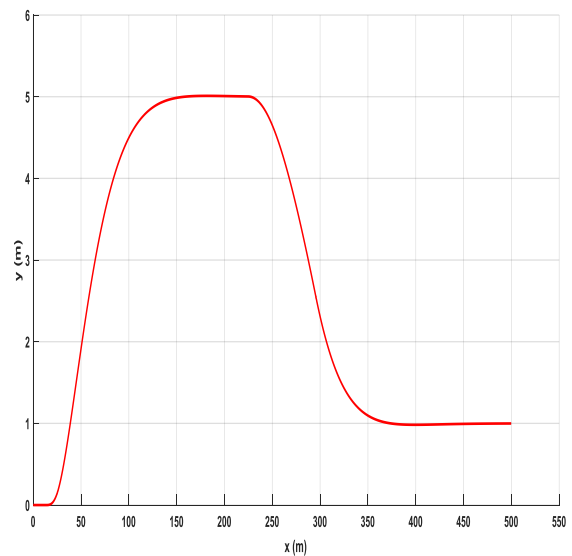


Fig. 6: SDC trajectory



Fig. 7: The visual display of SDC motion

7 Conclusions

A simulation model for ISEAUTO SDC was obtained and tested using Simulink software.

The proposed methodology can be used to improve the design of the SDC simulation model for applications that involve various control problems.

After setting up the given scenario, we simulate the two lanes change maneuver and get a realistic and expressive 3D video. The simulation results show an impressive quality of LQR control for the proposed SDC model, ensuring the smoothness and safety of the SDC motion trajectories. It can be expected also that the obtained control system may be applied easily to other types of SDCs as well.

The benefits of his research lie in the fact that the soft and reliable trajectory of the SDC can be realized during the transition between two selected lines of motion.

The limitations of this study were revealed in the fact that it is impossible to obtain the desired control time from the output coordinate and, thus, it is impossible to change the boundaries of the SDC safe movement zone.

The suggested improvement of this work can be the development of a control system for the MDC, which will allow obtaining the desired values for the time of regulation of the output coordinate and the possibility of a given change in the safety zone when the MDC is moving.

A future direction may be research related to the development of a simulation model that will consider the influence of weather conditions on the movement of the SDC on the base of the ISEAUTO platform in TalTech in a smart city environment.

Acknowledgment:

This work was partially supported by H 2020 grant No. 856602 and ERDF grant No. 2014 - 2020. 4. 01. 20 - 0289.

References:

- [1] V. Tsiatsis, S. Karnouskos, J. Holler, D. Boyle, and C. Mulligan, "Autonomous vehicles and systems of cyber-physical systems," in *Internet of Things: Technologies and Applications for a New Age of Intelligence*, London: Academic Press, 2019, pp. 209–305.
- [2] N. A. Stanton, R. Stewart, D. Harris, and R. J. Houghton, "Distributed situation awareness in dynamic systems: theoretical development and application of an ergonomics methodology," *Ergonomics*, vol. 49, October 2006, pp. 1287–1311.
- [3] R. Sell, M. Leier, A. Rassõlkin, and J.-P. Ernits, "Autonomous last mile shuttle ISEAUTO for education and research," *International Journal of Artificial Intelligence and Machine Learning*, vol. 10, June 2020, pp. 18–30.
- [4] K. Kalda, R. Sell, and R.-M. Soe, "Self-driving shuttle bus use case in city of Tallinn", Proc. IOP Conference Series: Materials Science and Engineering/ Modern Materials and Manufacturing, MMM 2021, pp. 1–6, 2021.
- [5] I. Astrov, *Neural Network Control of Vehicles: Modeling and Simulation*. Hauppauge, New York, USA: Nova Science Publishers, 2022.
- [6] X. Zhang, Y. Fan, H. Liu, Y. Zhang, and Q. Sha, "Design and implementation of autonomous underwater vehicle simulation system based on MOOS and unreal engine," *Electronics*, vol. 12, Article #3107, 2023.
- [7] P. Zhou, S. Lai, J. Cui, and B. M. Chen "Formation control of unmanned rotorcraft systems with state constraints and inter-agent collision avoidance," *Autonomous Intelligent Systems*, vol. 3, Article #4, 2023.
- [8] Y. Yamada, A. S. M. Bakibillah, K. Hashikura, M. A. S. Kamal, and K. Yamada, "Autonomous vehicle overtaking: modeling and an optimal trajectory generation scheme," *Sustainability*, vol. 14, Article #1807, 2022.
- [9] Y. Chen, G. Zhang, Y. Zhuang, and H. Hu, "Autonomous flight control for multi-rotor UAVs flying at low altitude," *IEEE Access*, vol. 7, January 2019, pp. 42614–42625.
- [10] M. Bellone, A. Ismailogullari, T. Kantala, S. Mäkinen, R.-M. Soe, and M. Kyyrö, "A cross-country comparison of user experience of public autonomous transport," *European*

Transport Research Review, vol.13, Article # 19, 2021.

- [11] I. Astrov, A. Udal, H. Pikner, and E. Malayjerdi, "A model-based LQR control of an obstacle avoidance maneuver of a self-driving car", Proc. IEEE 20th Jubilee World Symposium on Applied Machine Intelligence and Informatics, SAMI 2022, pp. 473–478, 2022.
- [12] M. G. Plessen, D. Bernardini, H. Esen, and A. Bemporad, "Spatial-based predictive control and geometric corridor planning for adaptive cruise control coupled with obstacle avoidance," *IEEE Trans. Control Systems Technology*, vol. 26, no. 1, pp. 38–50, 2018.
- [13] I. Astrov, A. Udal, and M. Jaanus, "A model-based adaptive control of an autonomous driving car for lane change maneuver", Proc. 44th International Convention on Information, Communication and Electronic Technology/ International Conference on Robotics Technologies and Applications, MIPRO RTA 2021, pp. 1330–1335, 2021.
- [14] ISEAUTO, [Online], <https://digi.geenius.ee/teemad/iseauto/> (Accessed Date: 12 May, 2023).
- [15] Parallelepiped rotating about the axis of its larger faces, [Online], https://www.sasview.org/docs/old_docs/4.2.2/user/models/parallelepiped.html (Accessed Date: 12 May, 2023).
- [16] G. Baffet, A. Charara, and D. Lechner, "Estimation of vehicle sideslip, tire force, and wheel cornering stiffness," *Control Engineering Practice*, vol. 17, November 2009, pp. 1255–1264.

Appendix

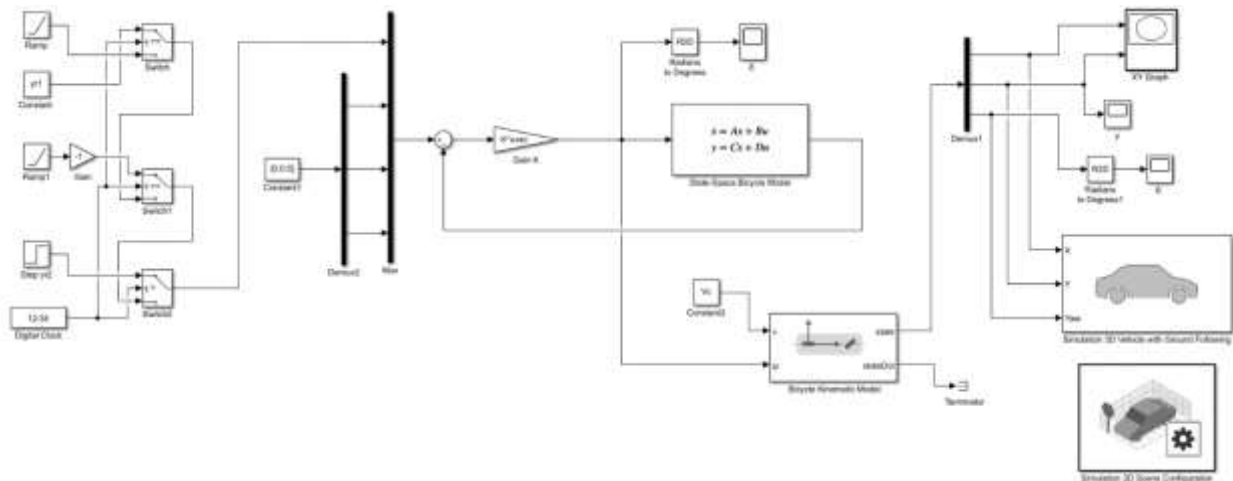


Fig. 2: Control system for SDC

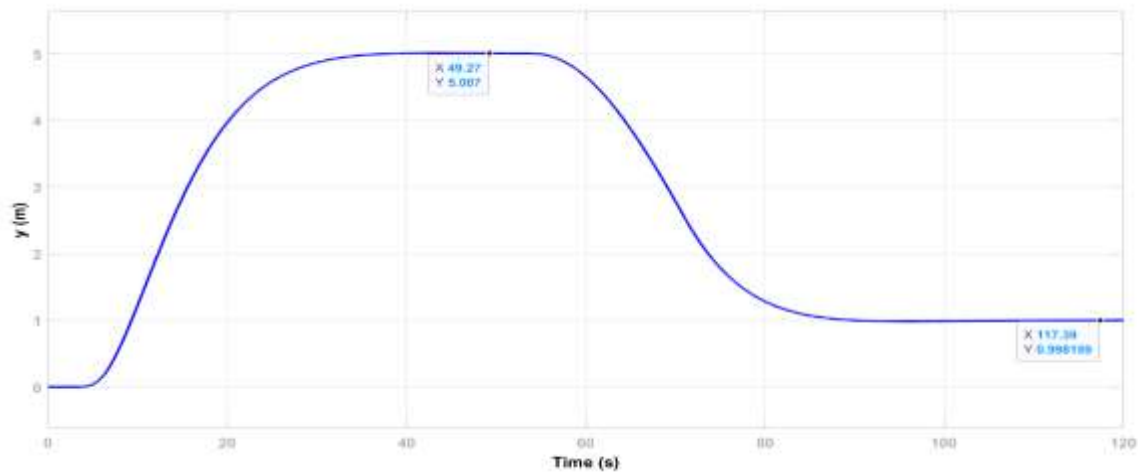


Fig. 5: Coordinate y of SDC

Contribution of Individual Authors to the Creation of a Scientific Article (Ghostwriting Policy)

The author completed all stages of this research.

Sources of Funding for Research Presented in a Scientific Article or Scientific Article Itself

This work was partially supported by H 2020 grant No. 856602 and ERDF grant No. 2014 - 2020. 4. 01. 20 - 0289.

Conflict of Interest

For the author no conflict of interest regarding the content of this paper.

Creative Commons Attribution License 4.0 (Attribution 4.0 International, CC BY 4.0)

This article is published under the terms of the Creative Commons Attribution License 4.0

https://creativecommons.org/licenses/by/4.0/deed.en_US